

Integrated approach to the assessment of long range correlation in time series data

Govindan Rangarajan*

Department of Mathematics and Centre for Theoretical Studies, Indian Institute of Science, Bangalore 560 012, India

Mingzhou Ding†

Center for Complex Systems and Brain Sciences, Florida Atlantic University, Boca Raton, Florida 33431

(Received 22 September 1999; revised manuscript received 21 January 2000)

To assess whether a given time series can be modeled by a stochastic process possessing long range correlation, one usually applies one of two types of analysis methods: the spectral method and the random walk analysis. The first objective of this work is to show that each one of these methods used alone can be susceptible to producing false results. We thus advocate an integrated approach which requires the use of both methods in a consistent fashion. We provide the theoretical foundation of this approach and illustrate the main ideas using examples. The second objective relates to the observation of long range anticorrelation (Hurst exponent $H < 1/2$) in real world time series data. The very peculiar nature of such processes is emphasized in light of the stringent condition under which such processes can occur. Using examples, we discuss the possible factors that could contribute to the false claim of long range anticorrelations, and demonstrate the particular importance of the integrated approach in this case.

PACS number(s): 05.40.Fb, 05.45.Tp

I. INTRODUCTION

Random processes with long range power law correlation have been observed in a variety of fields including economics, geosciences, physics, and biology [1–9]. There are roughly two types of tools used in assessing the presence of such correlations in time series data: spectral domain methods represented by power spectrum analysis [1,9], and random walk methods in the time domain represented by the rescaled range analysis [1,9,10]. Often these two types of tools are applied singly to a given data set. In Sec. II of this paper, we point out the pitfalls of this approach through a series of examples, and advocate an integrated approach which requires a consistent application of both types of methods.

Long range correlations are characterized by a quantity called the Hurst exponent H . When $H > 1/2$ the process is said to have positive long range correlation or persistence, while $H < 1/2$ means the process has long range anticorrelation or antipersistence. When $H = 1/2$ we say that the process has short range correlation. In Sec. III of this paper we present the condition for $H < 1/2$, and discuss how this stringent condition can be corrupted in real world data. We then proceed to demonstrate the significance of the integrated approach in this case, and analyze the reason underlying the many reported examples of $H < 1/2$.

II. AN INTEGRATED APPROACH TO THE ASSESSMENT OF LONG RANGE CORRELATION IN TIME SERIES

In this section, we argue that an integrated approach is required to assess long range correlations in times series.

*Also associated with the Jawaharlal Nehru Center for Advanced Scientific Research, Bangalore, India. Electronic address: rangaraj@math.iisc.ernet.in

†Electronic address: ding@walt.ccs.fau.edu

First, we derive the relationships between the power law exponents obtained from analyzing the time series using three different tools—spectral, autocorrelation, and rescaled range analyses. Then we demonstrate through examples that the use of spectral method or the rescaled range method alone can produce erroneous results. The autocorrelation method is not considered, since it is often difficult to use in practice.

A. Theoretical considerations

Consider a stationary stochastic process in discrete time, $\{\xi_k\}$, with $\langle \xi_k \rangle = 0$ and $\langle \xi_k^2 \rangle = \sigma^2$. Here $\langle \rangle$ denotes ensemble average. If the autocorrelation function $C(n) = \langle \xi_k \xi_{k+n} \rangle$ scales with the lag n as

$$C(n) \sim n^{-\beta} \quad (1)$$

for large n , where $0 < \beta < 1$, then $\{\xi_k\}$ is called a long range correlated or long memory process [9]. The reason for the latter term is that $C(n)$ decays so slowly that $\sum_{n=1}^N C(n)$ diverges as $N \rightarrow \infty$. (The case of $\beta > 1$ will be treated in Sec. III of this paper.)

The correlation structure of $\{\xi_k\}$ can be conveniently measured by the power spectrum, which is defined as [11]

$$S(f) = C(0) + 2 \sum_{n=1}^{\infty} C(n) \cos(2\pi fn). \quad (2)$$

If $C(n)$ obeys the scaling relation in Eq. (1) then

$$S(f) \approx 2 \sum_{n=1}^{\infty} n^{-\beta} \cos(2\pi fn). \quad (3)$$

In this case, we show below that

$$S(f) \sim f^{-\alpha} \quad (4)$$

for small f where $\alpha = 1 - \beta$.

The proof of this relationship between α and β draws on well known results in trigonometric series theory [12]. Consider the Taylor expansion of the function $(1-y)^{-\delta-1}$,

$$(1-y)^{-\delta-1} = \sum_{n=0}^{\infty} A_n^{\delta} y^n, \quad (5)$$

where by definition we have $A_0^{\delta} = 1$ and, for $n \geq 1$,

$$A_n^{\delta} = \frac{(\delta+1)(\delta+2)\cdots(\delta+n)}{n!} \\ \approx \frac{n^{\delta}}{\Gamma(\delta+1)}.$$

This means

$$\sum_{n=1}^{\infty} n^{\delta} y^n \approx \Gamma(\delta+1)[(1-y)^{-\delta-1} - 1]. \quad (6)$$

Replacing $\delta = -\beta$, $y = re^{i2\pi f}$, and $0 \leq r < 1$ in the above equation leads to

$$\sum_{n=1}^{\infty} n^{-\beta} r^n e^{i2\pi n f} \approx \Gamma(1-\beta)[(1-re^{i2\pi f})^{\beta-1} - 1]. \quad (7)$$

Letting $r \rightarrow 1$ and $f \rightarrow 0$, and taking the real part, we obtain

$$\sum_{n=1}^{\infty} n^{-\beta} \cos 2\pi n f \approx \Gamma(1-\beta)(2\pi f)^{\beta-1} \cos[\pi(1-\beta)/2]. \quad (8)$$

Substituting this into Eq. (3) yields

$$S(f) \approx 2\Gamma(1-\beta)(2\pi f)^{\beta-1} \cos[\pi(1-\beta)/2] \\ \sim f^{\beta-1}.$$

Comparing the above with Eq. (4), we obtain $\alpha = 1 - \beta$.

Another way to assess the correlation structure of $\{\xi_k\}$ is to convert the stationary process to a random walk by using partial sums, $R_1 = \xi_1$, $R_2 = \xi_1 + \xi_2$, \dots , $R_n = \xi_1 + \xi_2 + \dots + \xi_n$, \dots , where R_n is the position of the walker at time n . The mean range of the random walk trajectory as a function of time bears specific relations with the scaling relation [Eq. (1)]. For the ease of analytical evaluation we consider the mean square displacement as a measure of the range of the random walk, which is defined as

$$\langle R_n^2 \rangle = \sum_{i=1}^n \langle \xi_i^2 \rangle + 2 \sum_{s=1}^{n-1} (n-s) C(s) \\ = n\sigma^2 + 2n \sum_{s=1}^{n-1} C(s) - 2 \sum_{s=1}^{n-1} s C(s). \quad (9)$$

Let $C(s)$ obey the scaling law in Eq. (1). The sums in the above equation are estimated as

$$\sum_{s=1}^{n-1} C(s) \sim \sum_{s=1}^n s^{-\beta} \sim \int_1^n s^{-\beta} \sim n^{1-\beta} \quad (10)$$

and

$$\sum_{s=1}^{n-1} s C(s) \sim \sum_{s=1}^n s^{1-\beta} \sim \int_1^n s^{1-\beta} \approx n^{2-\beta}. \quad (11)$$

For $0 < \beta < 1$, this means

$$\langle R_n^2 \rangle \sim n^{2-\beta} \quad (12)$$

for large n . Conventionally, the mean square displacement is characterized by the Hurst exponent H as

$$\langle R_n^2 \rangle \sim n^{2H}, \quad (13)$$

where

$$H = (2 - \beta)/2 = (1 + \alpha)/2. \quad (14)$$

Thus we obtain a set of consistent relations between the scaling exponents α , β , and H .

B. Examples

As shown in Sec. II A, the scaling exponents obtained from spectral analysis and from random walk analysis must be consistent through Eq. (14). We first provide three examples of two simulated correlated processes and one experimental long range correlated process demonstrating this consistency. Then we proceed to show that the spectral method or the random walk method used alone can be susceptible to artifacts in the data and produce erroneous results. The combination of the two methods can often detect such artifacts through inconsistencies with Eq. (14).

The random walk analysis tool that we will use in this paper is the rescaled range analysis [1,5]. A brief description of this method follows. For a given data set $\{\xi_i\}$, consider the sum $L(n,s) = \sum_{i=1}^s \xi_{n+i}$, where $L(n,s)$ can be regarded as the position of a random walk after s steps. Define the trend-corrected range $R(n,s)$ of the random walk as

$$R(n,s) = \max\{L(n,p) - pL(n,s)/s, 1 \leq p \leq s\} \\ - \min\{L(n,p) - pL(n,s)/s, 1 \leq p \leq s\}. \quad (15)$$

Let $S^2(n,s)$ denote the variance of the data set $\{\xi_{n+i}\}_{i=1}^s$. If the data has long range correlation, the average rescaled statistic $Q(s) = \langle R(n,s)/S(n,s) \rangle_n$ (where $\langle \rangle_n$ denotes the average over n) scales with s as a power law for large s ,

$$Q(s) \sim s^H, \quad (16)$$

where H is the Hurst exponent introduced earlier. This power law manifests itself as a straight line in the log-log plot of $Q(s)$ versus s . Spectral analysis was done using fast Fourier transform, and the Bartlett window was employed [13].

1. Genuine long range Correlated processes

To generate a process whose spectral density scales with the frequency f as a power law $f^{-\alpha}$, we start with a realization of a discrete zero mean white Gaussian noise process $\{\xi_k\}$, $k=0,1,\dots,N-1$, with variance σ^2 . Using Fourier transform, we obtain

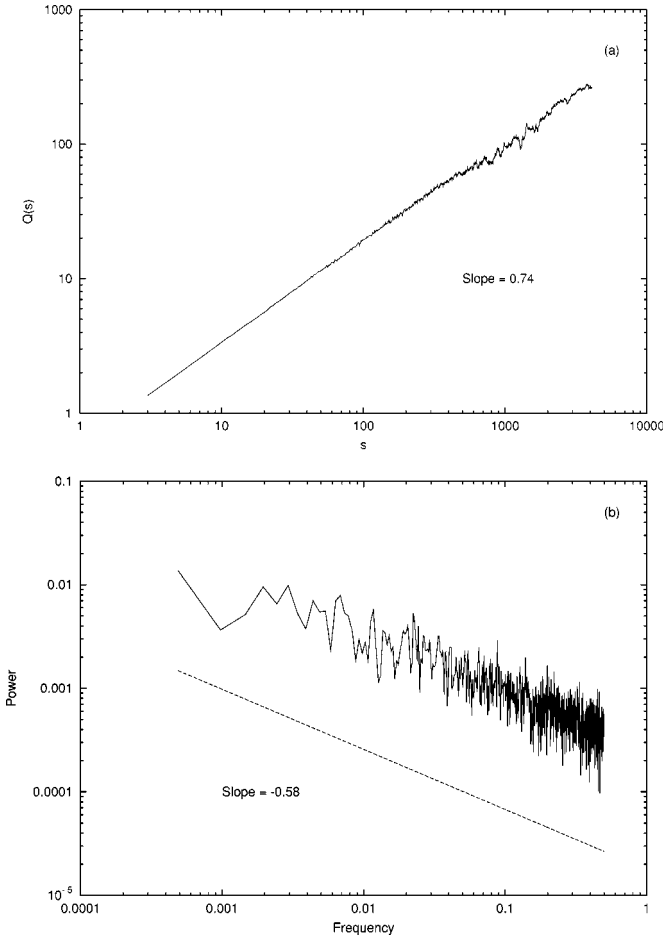


FIG. 1. (a) Log-log plot of the rescaled range statistic $Q(s)$ against the window size s for a true long range correlated process with $\alpha=0.6$, variance 0.25, and a long data set of 8192 points. (b) Spectral density of the same data.

$$\Gamma_k = \sum_{n=0}^{N-1} \xi_n \exp(-i2\pi nk/N), \quad k=0,1,\dots,N-1. \tag{17}$$

Next we multiply Γ_k by the factor $f^{-\alpha/2}=(k/N)^{-\alpha/2}$ to obtain the scaled quantity Γ'_k . (Both Γ_k and Γ_{N-k} are multiplied by the same factor since we want a real-valued time series.) Finally we perform an inverse Fourier transform to obtain

$$x_n = \frac{1}{N} \sum_{k=0}^{N-1} \Gamma'_k \exp(2\pi nk/N), \quad n=0,1,\dots,N-1. \tag{18}$$

The discrete process x_n , by construction, has a mean power spectrum that scales as $f^{-\alpha}$ with the frequency. The variability around the mean spectrum is provided by the white noise process.

For our first example we generated a long range correlated process using the above construction with $\alpha=0.6$ and variance 0.25. The first data set has 8192 points. When we apply rescaled range analysis to this data, we obtain a Hurst exponent $H=0.74$ [see Fig. 1(a)]. The power spectrum ex-

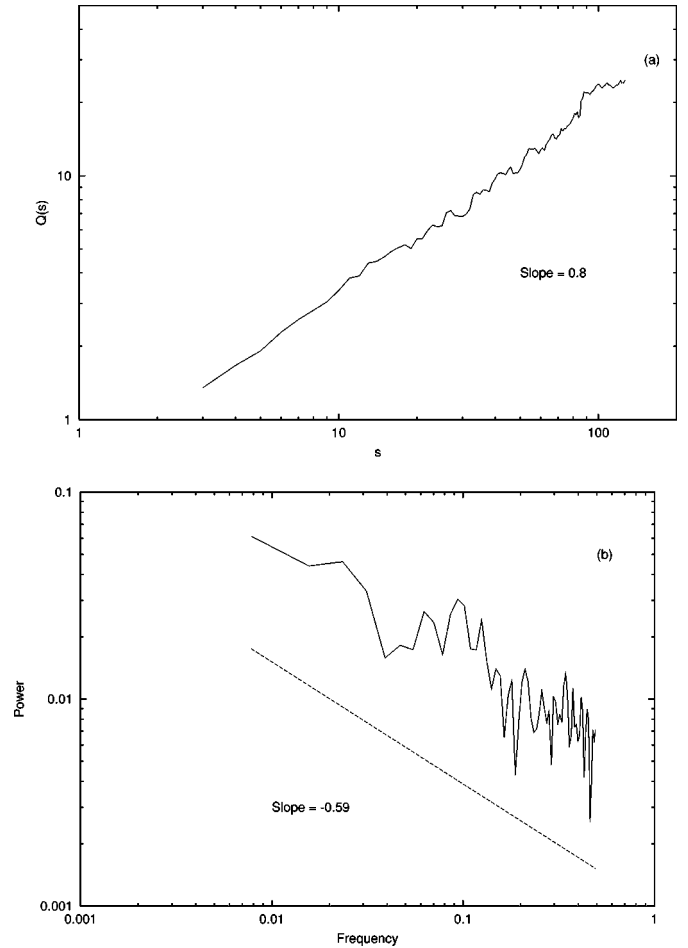


FIG. 2. (a) Log-log plot of the rescaled range statistic $Q(s)$ against the window size s for a true long range correlated process with $\alpha=0.6$, variance 0.25, and a short data set of 256 points. (b) Spectral density of the same data.

hibits a power law behavior (by construction) with $\alpha=0.58$ [see Fig. 1(b)]. Note that these values are consistent with Eq. (14) [14].

Next we truncated the above time series data to obtain a short data set with only 256 points. The results from rescaled range and power spectrum analyses are shown in Figs. 2(a) and 2(b), respectively. Again these two results are consistent with one another. This illustrates the fact that when you have a process with genuine long range correlation, even a short data set is often sufficient to reveal this property.

As a second example, we consider a different type of long range correlated process – a fractional auto regressive integrated moving average (ARIMA) $(0,d,0)$ process [9] with $0 \leq d < 0.5$. It can be shown that the autocorrelation function $C(n)$ for this process scales with lag n as $C(n) \sim n^{2d-1}$. Thus from Eq. (14), $\beta=1-2d$ and $H=d+0.5$. The fractional ARIMA $(0,d,0)$ process for $d=0.25$ ($H=0.75$) was generated [15] using its known autocovariance function [9]. The results from rescaled range analysis and spectral analysis of this data, shown in Figs. 3(a) and 3(b) are mutually consistent with one another [cf. Eq. (14)].

The final example analyzes the data from a finger tapping experiment involving the human sensorimotor coordination [7]. In this experiment, subjects cyclically tapped their index finger against a computer key in synchrony with a periodic

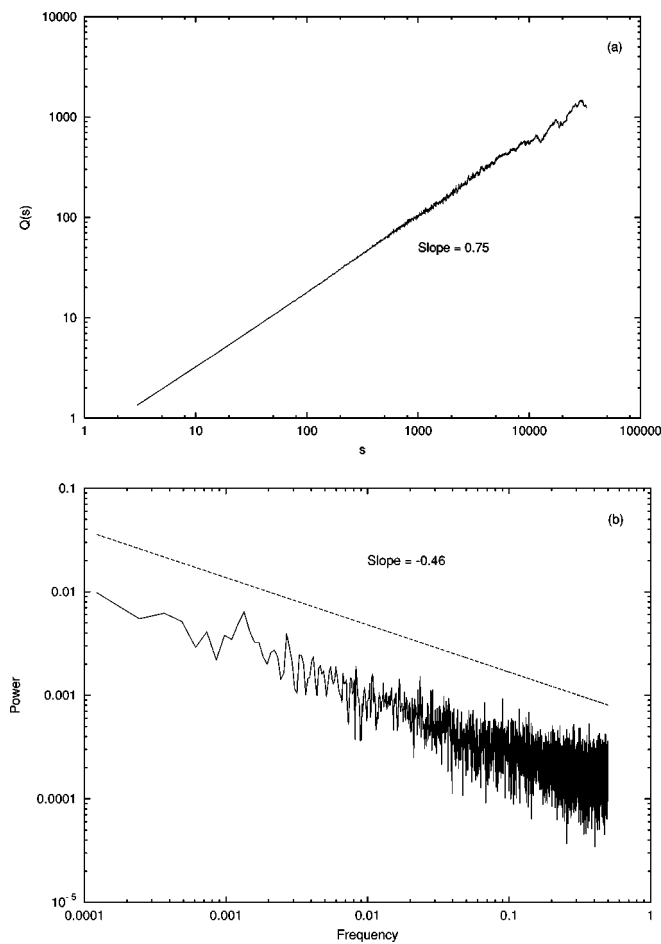


FIG. 3. (a) Log-log plot of the rescaled range statistic $Q(s)$ against the window size s for a fractional ARIMA(0, d ,0) process with $d=0.25$. (b) Spectral density of the same data.

series of auditory beeps, delivered through a headphone. The data collected were the synchronization or tapping errors defined as the time between the computer recorded response time and the metronome onset (see Ref. [7] for further details). Here we analyze the synchronization error time series from this experiment using rescaled range and spectral analyses. The results, exhibited in Figs. 4(a) and 4(b), are again mutually consistent demonstrating that the error time series has long range correlations [7].

2. Failures of the rescaled range analysis

In this section, we consider various situations where rescaled range analysis used alone can give wrong results. As our first example, we consider the superposition of an exponential trend over a white noise process. (See, Ref. [16] for more examples in this area.) Specifically, we generated the following discrete process

$$x_k = \exp(-0.01k) + \xi_k, \quad k = 1, 2, \dots, \quad (19)$$

where $\{\xi_k\}$ is a white noise process with zero mean and variance 0.16. A total of 8192 points were generated. This example can be realized in situations where the process under investigation has an exponentially decaying transient, and one does not discard the initial portion of the data (containing this transient) while recording it.

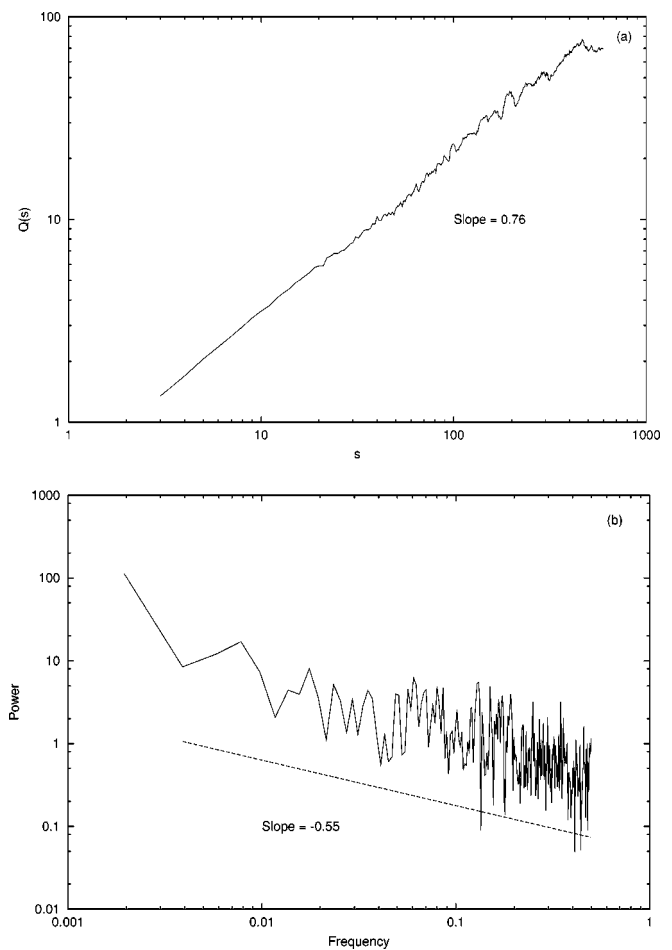


FIG. 4. (a) Log-log plot of the rescaled range statistic $Q(s)$ against the window size s for the synchronization error time series data from the finger tapping experiment. (b) Spectral density of the same data.

When the above process is subject to rescaled range analysis, we obtain a Hurst exponent equal to 0.75 [see Fig. 5(a)], indicating long range correlation where there is none. On the other hand, the power spectrum is flat [see Fig. 5(b)], and does not show any power law behavior. This inconsistency between the spectral method and rescaled range method serves as a warning sign pointing to the need for further more careful examination of the data.

As our second example, we consider the following autoregressive (AR) process of order one [AR(1)] [11]:

$$x_k = \lambda x_{k-1} + \xi_k, \quad k = 1, 2, \dots, \quad (20)$$

where $\{\xi_k\}$ is a zero mean white noise process with variance 0.25, and the coefficient λ is close to 1 (0.9 in our case). The autocorrelation function of the x process decays exponentially: $C(k) \sim \lambda^k$. This means there is no long range correlation in the x process. However, as shown in Fig. 6(a), the rescaled range analysis of the above process (with 1024 points) indicates the presence of long range correlation by producing $H=0.76$. The power spectrum [Fig. 6(b)], on the other hand, exhibits a flattening trend at low frequencies and contradicts the result from the rescaled range analysis. Even if one misses this flattening trend and fits a straight line to the remaining portion of the spectrum on a log-log scale, we

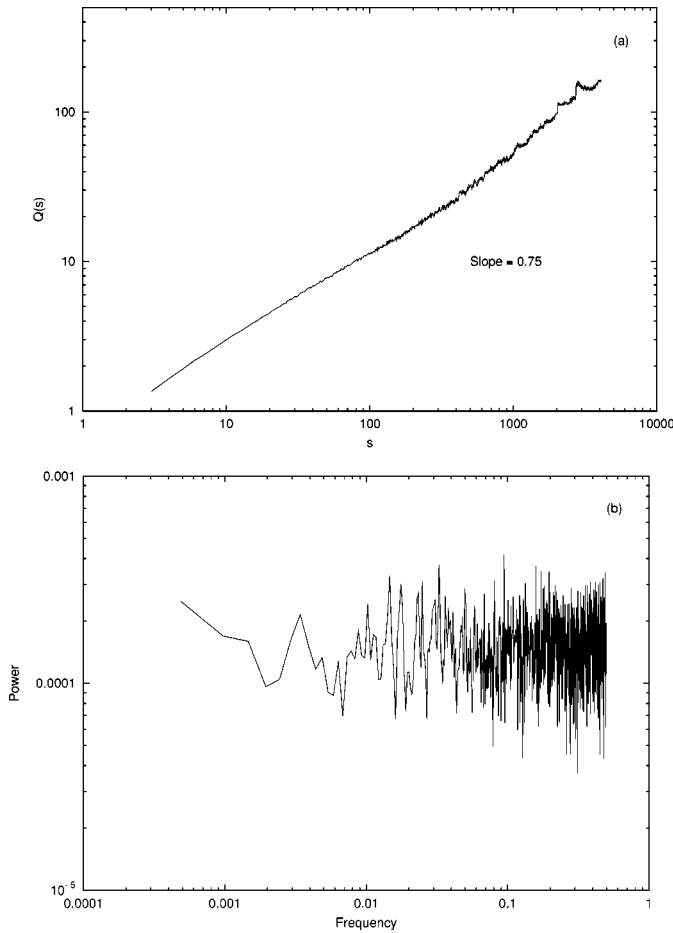


FIG. 5. (a) Log-log plot of the rescaled range statistic $Q(s)$ against the window size s for the superposition of an exponential trend over a white noise process. (b) Spectral density of the same data.

obtain a value for α equal to -1 . Here the consistency relation $H \approx (1 + \alpha)/2$ is not satisfied, thus indicating the absence of long range correlations.

As our third example, we again consider an AR(1) process [cf. Eq. (20)], but this time with the coefficient λ close to -1 (-0.9 in our case). In this example, the application of the rescaled range analysis gives a Hurst exponent $H = 0.33$ [Fig. 7(a)]. Naively, this Hurst value can be interpreted as an indicator of long range “antipersistence” [1]. As before, the power spectrum contradicts this result [see Fig. 7(b)], and shows a flattening trend in the low frequencies. This observation is further strengthened by analyzing a long data set (100 000 points) using rescaled range analysis. The results [see Fig. 7(c)] show that H approaches a value of 0.5 as the data set becomes longer. In Sec. III of this paper we will discuss in more detail processes with the Hurst exponent $H < 1/2$.

We would like to make one point regarding the application of the surrogate data analysis [17], which is often used in combination with many analysis methods to strengthen their results by demonstrating that a completely random process could not have exhibited the observed results. We show below that this is not fool proof when used in conjunction with rescaled range analysis. We have already seen in the second example above that rescaled range analysis indicates

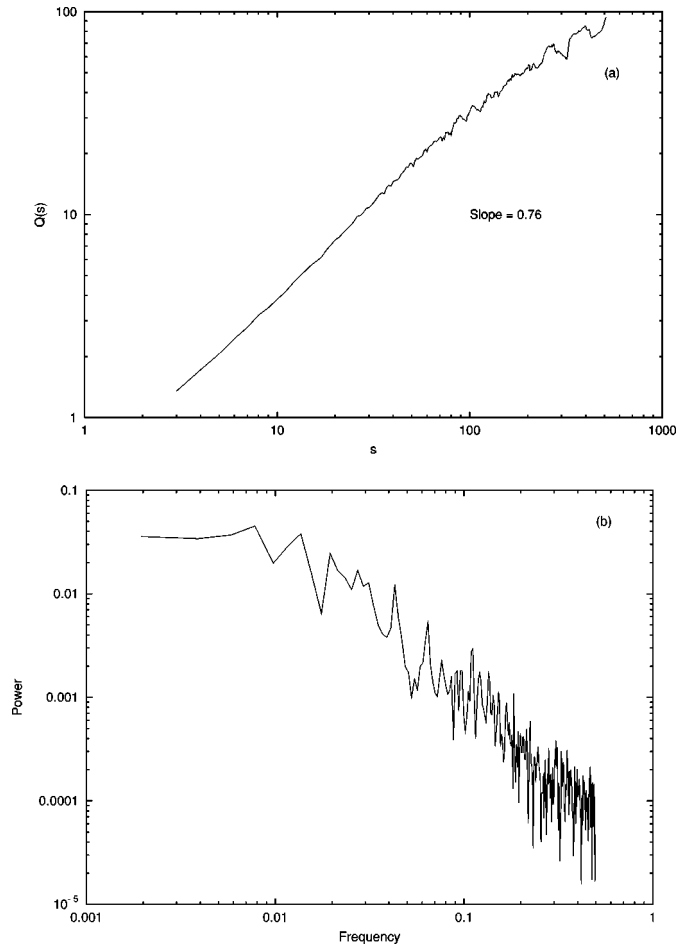


FIG. 6. (a) Log-log plot of the rescaled range statistic $Q(s)$ against the window size s for an AR(1) process with $\lambda = 0.9$. (b) Spectral density of the same data.

the presence of long range correlation in the AR(1) process (with $\lambda = 0.9$) where there is none. We now apply surrogate data analysis by shuffling the data randomly and reapplying rescaled range analysis to the shuffled data sets. Figure 8 shows comparison between the Hurst exponent obtained from the unshuffled original data with the average value of Hurst exponents obtained from five realizations of randomly shuffled data. We see that the shuffled data gives an average value of H around 0.5 as compared to 0.76 for the original data. The two results are well separated. Therefore, the application of surrogate data analysis would indicate that the result obtained by rescaled range analysis of the original data is correct, indicating the presence of long range correlation. This is obviously a false conclusion. This example demonstrates that surrogate data analysis cannot be used indiscriminately for this type of problems.

3. Failure of the power spectrum analysis

Here we give an example where the use of power spectrum analysis with inappropriate parameters can lead to wrong results. If we investigate the genuine long range process introduced above using the power spectrum analysis with a Parzen window and $M = 20$ (that is, with a lot of smoothing) [11], then we obtain the spectrum given in Fig. 9. This power spectrum shows a flat portion at low frequencies,

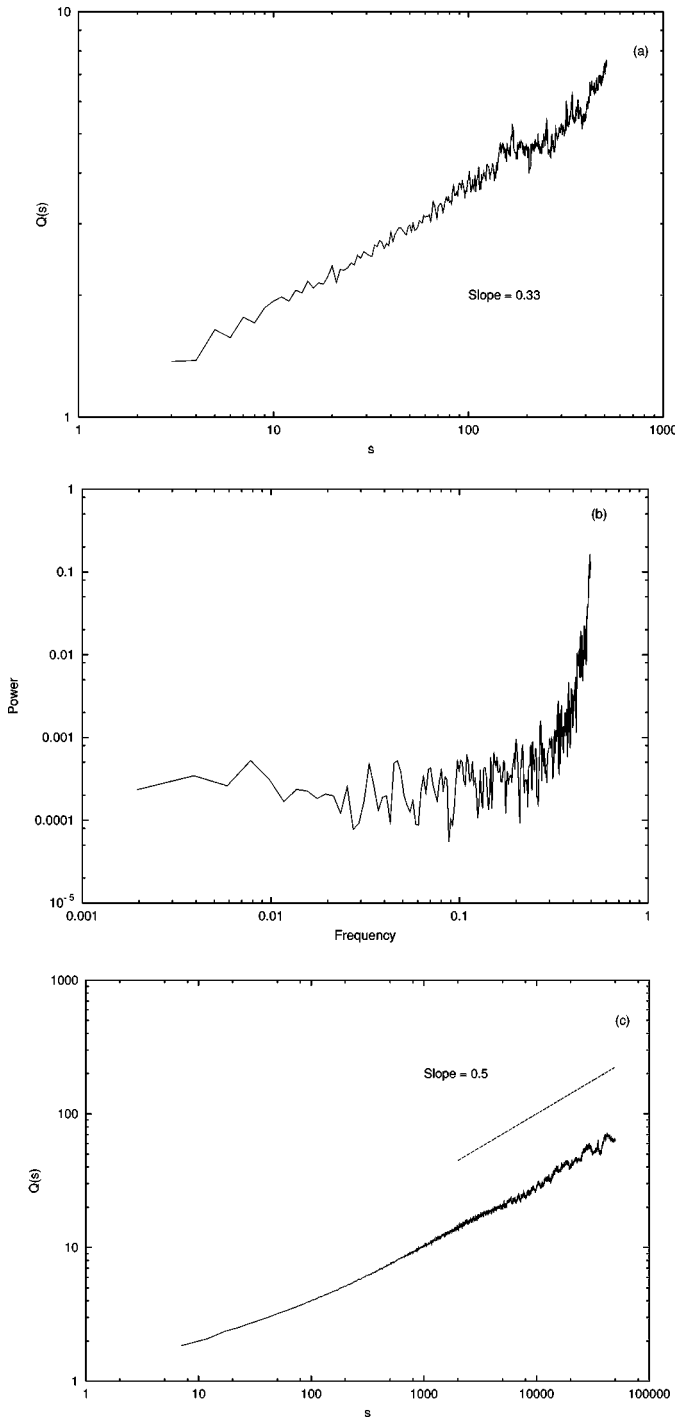


FIG. 7. (a) Log-log plot of the rescaled range statistic $Q(s)$ against the window size s for an AR(1) process with $\lambda = -0.9$, variance 0.25, and 1024 data points. (b) Spectral density of the same data. (c) Log-log plot of the rescaled range statistic $Q(s)$ against the window size s for the same process but with 100 000 points.

indicating wrongly the absence of long range correlations. This is not a problem with power spectrum analysis per se, but is an example of using it with inappropriate parameters. We do not run into such problems with rescaled range analysis, since it does not have such free parameters that can be wrongly “tuned.” The above example is not as artificial as it seems, since canned power spectrum analysis routines are often used in data analysis without proper thought going into

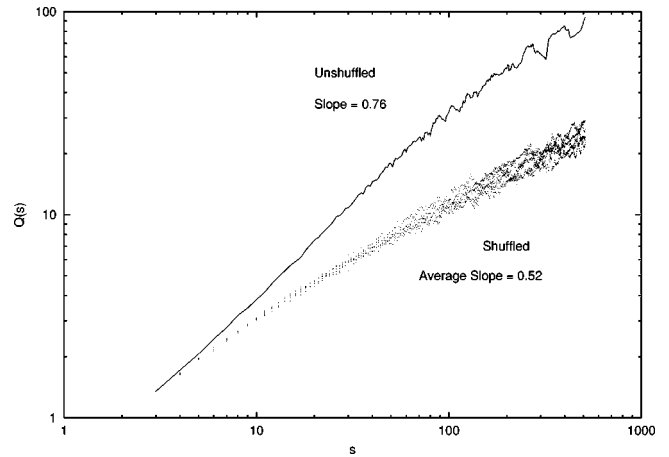


FIG. 8. Comparison between the Hurst exponent obtained from the unshuffled original data of the AR(1) process (with $\lambda = 0.9$) and the average value of Hurst coefficients obtained from five realizations of the above data, randomly shuffled.

the choice of input parameters. In this case the inconsistencies between the two analysis methods will prompt more careful examinations of the methods employed.

4. Failures of the combined use of rescaled range and power spectrum analysis

All the above examples illustrate the fact that one should not rely on a single tool to analyze time series data. An integrated approach requiring the consistent use of several available tools is more desirable. But even an integrated approach is not foolproof as we show below.

Consider a process that is the superposition of AR(1) processes. In particular, we consider a variable that is the sum of the following five independent processes:

$$x_k = \lambda x_{k-1} + \xi_k, \quad k = 1, 2, \dots, \quad (21)$$

where the coefficients λ for the individual processes are given by 0.99, 0.9, 0.4, 0.2, and 0.1, and the variances are given by 0.05, 0.1, 0.3, 0.4, and 0.5, respectively. In this case, for a relatively short data set of 256 points, both the rescaled range and power spectrum analyses indicate the

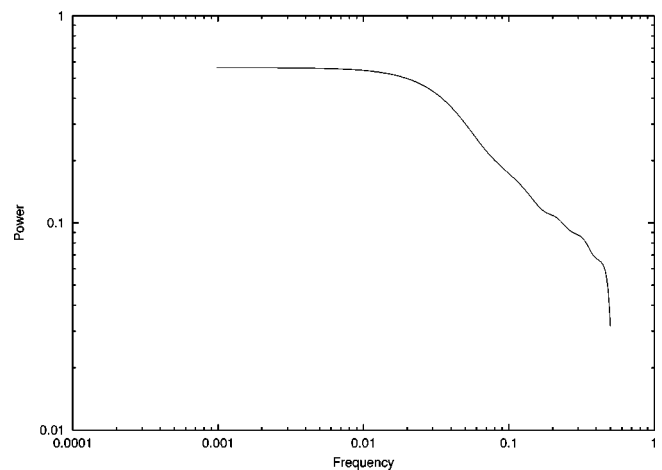


FIG. 9. Spectral density of the genuine long range correlated process considered in Fig. 1 using a Parzen window with $M = 20$.

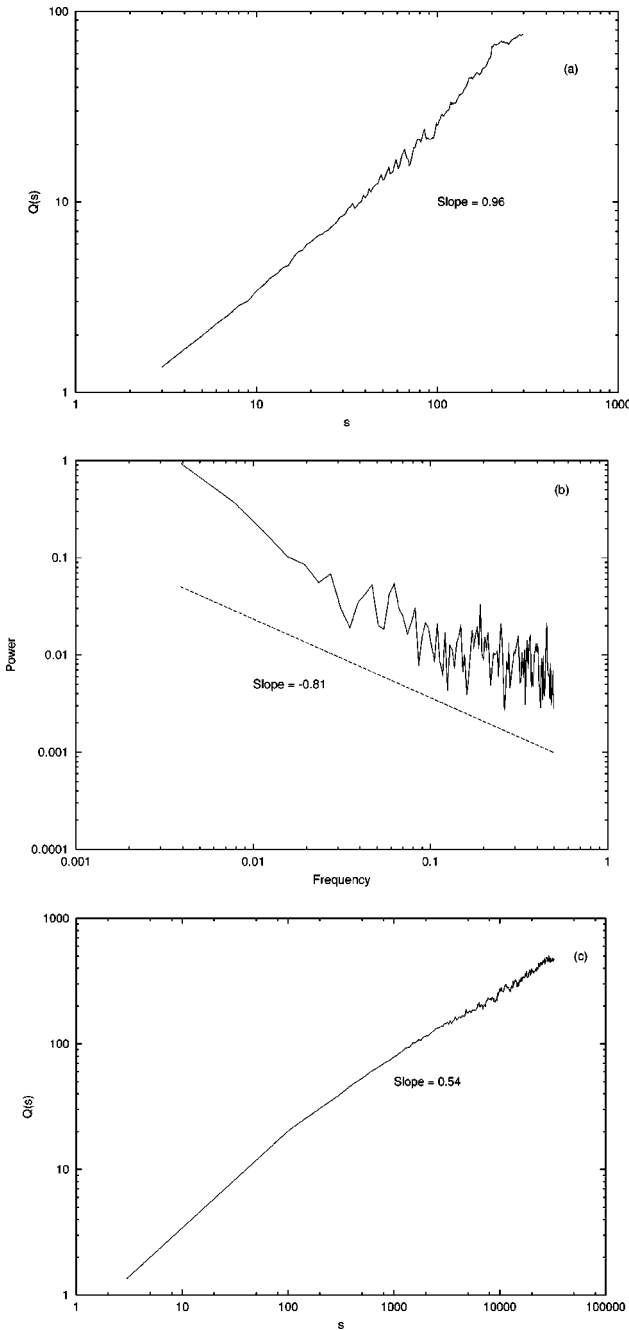


FIG. 10. (a) Log-log plot of the rescaled range statistic $Q(s)$ against the window size s for a superposition of five AR(1) process. (b) Spectral density of the same data. (c) $Q(s)$ versus s for a much longer data set from the same process.

presence of long range correlation in the data [see Figs. 10(a) and 10(b), respectively] by yielding $H=0.96$ and $\alpha=0.82$. Clearly, the results are consistent with $H \approx (1 + \alpha)/2$. But, for a much longer data set of 50 000 points we see the true Hurst exponent of $H=0.5$ in Fig. 10(c).

This example shows that even the superposition of a few AR(1) processes can mimic a long range correlated process for short data sets. Theoretically it is known that the superposition of an infinite number of AR(1) processes can, in some cases, give rise to a long range correlated process [18]. Even though an integrated approach using both rescaled range and power spectrum analyses can give spurious results,

consistent positive results from both these analyses at least indicates the presence of multiple time scales in the data set.

III. CONDITION FOR $H < 1/2$ AND ITS IMPLICATIONS FOR REAL WORLD DATA ANALYSIS

As mentioned earlier, rescaled range analysis [1,5] is often used in determining the presence of long range correlation in data sets. Results of rescaled range analyses are typically quantified using the Hurst exponent H ($0 < H < 1$). In principle, analysis of a data set can lead to any value of H between 0 and 1. In this section, we will argue that processes with $H < 1/2$ are rather special, in that they must satisfy the condition that the sum of the autocorrelation function be zero. Many physical processes are known to meet this condition [4]. However, this condition can be easily corrupted in real world data where noise unrelated to the physical process enters the measurement. We demonstrate the importance of the integrated approach in the proper diagnosis of processes with $H < 1/2$. We also discuss a common way in which a misjudgment of long range anticorrelation can occur. In this regard we identify the three contributing factors: (1) the variable being recorded is not fundamental (see below), (2) the data set is short, and (3) only a random walk type of analysis is employed.

A. Condition for $H < 1/2$

Refer to Eq. (9). Suppose that $C(s) \sim s^{-\beta}$. When $0 < \beta < 1$, we showed that both the second and third terms in the above equation diverge and scale with n as $\sim n^{2-\beta}$. Therefore, $\langle R_n^2 \rangle$ scales with n as $\sim n^{2-\beta}$ for large n , and this leads to $H > 1/2$ [cf. Eq. (14)]. For $\beta > 2$ [that is, for any $C(s)$ that decays faster than $C(s) \sim s^{-2}$], both sums in the above equation converge, and we generally obtain $H = 1/2$.

Thus the only remaining range of β is $1 < \beta < 2$. For such β the sum $\sum_{s=1}^{\infty} C(s)$ is finite. (Note that, strictly speaking, this type of process can no longer be termed a long memory process based on the definition in Sec. II A. But, since it has the potential of giving $H < 1/2$, we will still use the term ‘‘long range correlation.’’) Therefore the first two terms scale as $\sim n^1$. The sum $\sum_{s=1}^{n-1} sC(s)$ in the third term is evaluated to be

$$\sum_{s=1}^{n-1} sC(s) \sim n^{2-\beta}, \tag{22}$$

where $(2 - \beta) < 1$. This means that the rate of divergence of the third term is slower than the first two terms. Therefore, in the large n limit $\langle R_n^2 \rangle \sim n$, we would still observe $H = 1/2$. The only situation when this will not happen occurs when the following equation is precisely satisfied:

$$\sigma^2 + 2 \sum_{s=1}^{\infty} C(s) = \sum_{s=-\infty}^{s=\infty} C(s) = 0. \tag{23}$$

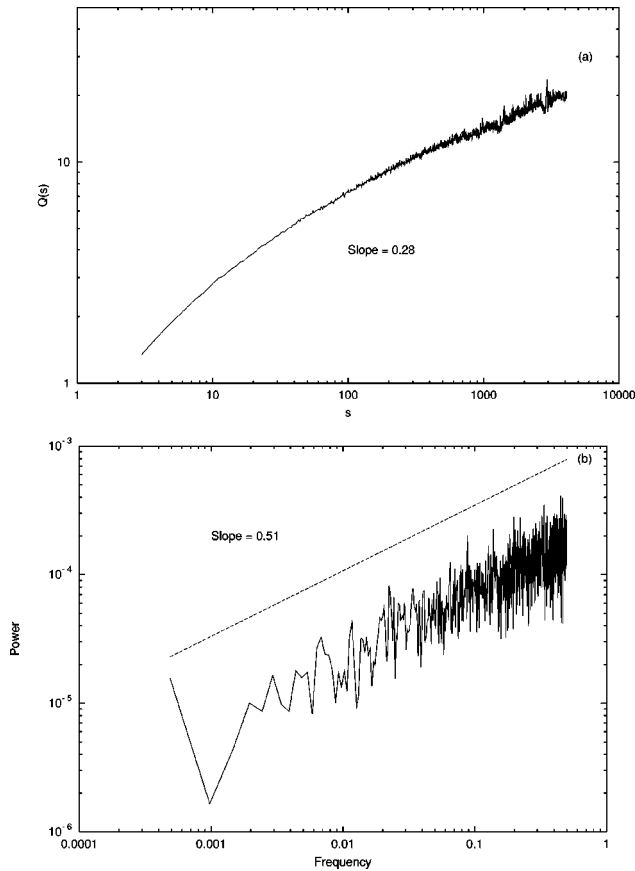


FIG. 11. (a) Log-log plot of the rescaled range statistic $Q(s)$ against the window size s for a true long range correlated process with $\alpha = -0.5$, variance 0.25, and a long data set (8192 points). (b) Spectral density of the same data.

In this case the first two terms in $\langle R_n^2 \rangle$ drop out giving $\langle R_n^2 \rangle \sim n^{2-\beta}$. Therefore, we obtain $H = (2 - \beta)/2$, which is smaller than $1/2$.

It is clear that for $H < 1/2$ to occur the process must meet a very stringent condition [Eq. (23)]. It has been shown that many physical systems satisfy this condition [4]. But, when such a physical system is subject to measurement, noise is an inevitable factor. For the noisy measurement it is likely that the equality in Eq. (23) no longer holds. The implication is that in the long run one may observe $H = 1/2$, and therefore not be able to correctly identify the underlying process. In what follows we show that the integrated approach advocated in Sec. II is again an essential tool in revealing strong clues as to the true nature of the physical process. Moreover, we will show that the integrated approach is also indispensable in guarding against misjudgment of $H < 1/2$ for systems where this is not true.

B. Integrated approach to noisy $H < 1/2$ data

For a genuine $H < 1/2$ process, Eq. (14) still holds, albeit α will be a negative number. We generated a $f^{-\alpha}$ process artificially using the procedure in Sec. II B 1. A value of $\alpha = -0.5$ was used. When the data are subject to rescaled range analysis, we obtain a value of $H = 0.28$ [see Fig. 11(a)]. The spectral analysis gives a power law curve with $\alpha = -0.5$ as expected [Fig. 11(b)]. We note the results of the

rescaled range and spectral analyses are mutually consistent in this case, since the application of Eq (14) gives a H value of 0.25.

Now we consider the effect of additive noise on the same data set. When noise is added, Eq. (23) is no longer strictly satisfied. Hence we would expect the Hurst exponent of the process to asymptotically approach $H = 0.5$ for long data sets. This is borne out by our numerical simulations. We start with the true long range correlated process described above ($H = 0.25$), and add Gaussian white noise to the data with variance 0.01. This simulates the effect of noisy measurement in experiments. Figure 12(a) shows the results of rescaled range analysis applied to the above process with 262,144 points. We see that H asymptotically tends to 0.5. As the variance of the added noise is increased, the $H = 0.5$ value is reached even faster. However, all is not lost. The integrated approach allows us to approximately recover the true process hidden by the noise. We start by truncating the data set which prevents the asymptotic limit for H being reached. Figs. 12(b) and 12(c) display the results of applying the integrated approach to the truncated data set with 8192 points [all other parameter values remain the same as in Fig. 12(a)]. We obtain an H value of 0.34 from rescaled range analysis, and the spectral analysis is consistent with this value. This consistency tells us that the data represent a true long range correlated process (the H value obtained is higher than that for the true process because of the added noise.) We comment that this consistency is in marked contrast to what was observed for the AR(1) process with $\lambda = -0.9$ (see Sec. II B). There, even though the H value was 0.33 for small data sets and rose to $H = 0.5$ for large data sets, the results of spectral analysis were completely inconsistent with this. This led us to conclude that there was no true long range correlated process in that example. The above examples again demonstrate that the integrated approach is very useful in revealing the true nature of a process represented by time series data.

C. Possible causes for false identification of $H < 1/2$

In the literature one often comes across reports where analysis of real world data, using the method of random walk alone, yield $H < 1/2$. The examples in Sec. II B show the shortcoming of using just one type of analysis method. Upon further examination we realize that there is a common thread in these reports that has to do with the fact that the data analyzed do not come from a fundamental process which we discuss below.

1. Notion of a fundamental process and data differencing

Consider a stationary process $\{\xi_k\}$. By definition a stationary process is not diffusive. In other words, $\langle \xi_k^2 \rangle$ is a constant. Consider the partial sum $R_n = \sum_{k=1}^n \xi_k$. If $\langle R_n^2 \rangle$ increases with n , that is, R_n is a diffusive process, we say that $\{\xi_k\}$ is a fundamental process. If the time series data coming from a fundamental process are subject to random walk type of analysis such as the rescaled range analysis, it can be trusted to correctly assess the corresponding Hurst exponent.

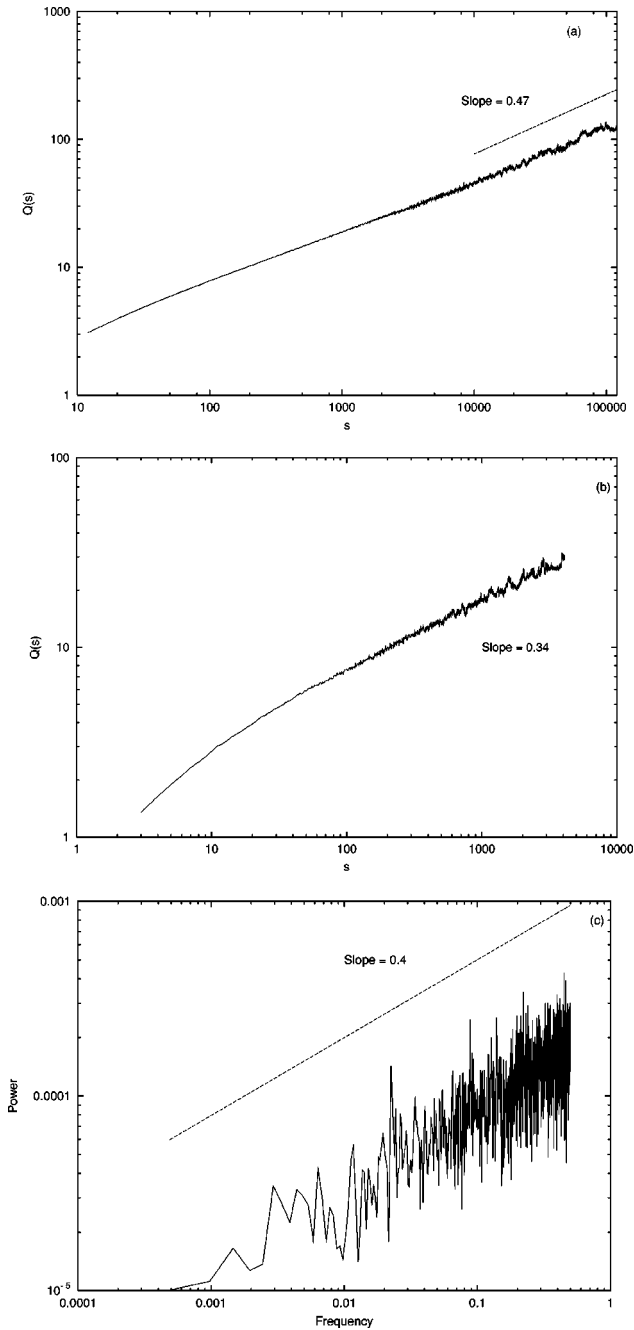


FIG. 12. (a) Log-log plot of the rescaled range statistic $Q(s)$ against the window size s for a true long range correlated process corrupted by added white noise with $\alpha = -0.5$, variance 0.25, and 262 144 points. The variance of added white noise is 0.01. (b) Same as above but with 8192 points. (c) Spectral density of the same process with 8192 points.

A differenced process refers to a process $\{\eta_k\}$ which is obtained by $\eta_k = \xi_{k+1} - \xi_k$. Clearly, $\{\eta_k\}$ is not a fundamental process, since its partial sums give $\{\xi_k\}$ which is not diffusive. This means if we input data from a differenced process into the rescaled range type of random walk analysis, we will not be able to assess the correlation properties of the original process, and possibly even be fooled by the appearance of the rescaled range plot (see below).

Differenced data can arise in practice in a number of ways. First, differencing is a commonly applied technique

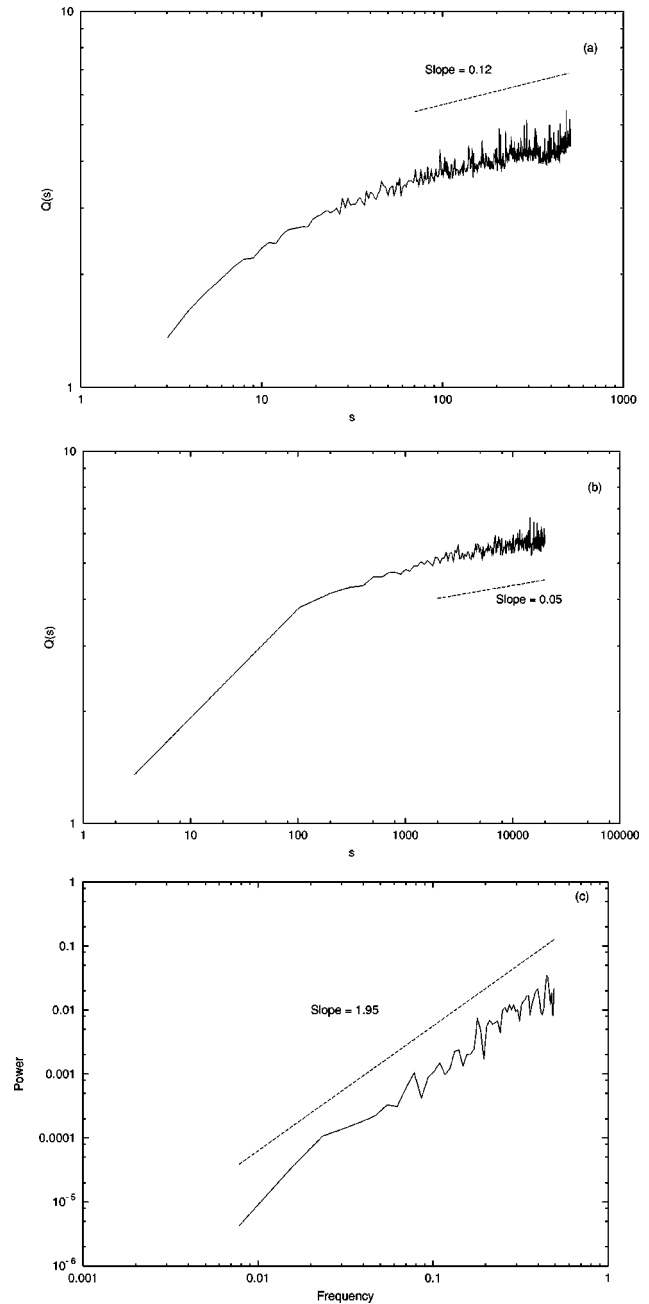


FIG. 13. (a) Log-log plot of the rescaled range statistic $Q(s)$ against the window size s for a differenced Gaussian white noise process with 1024 data points. (b) Same as above but with 40 000 data points. (c) Spectral density of the data in (a).

for trend removal [11]. Second, the measured physical variable is a derivative of another fundamental variable. We believe that the use of differenced data, in combination with a rescaled range type of analysis, underlies some of the reported cases of $H < 1/2$. Below we demonstrate this point by examples.

2. Gaussian white noise

Consider a Gaussian white noise process $\{\xi_k\}$. The partial sums of this process yield a diffusive Brownian motion with a Hurst exponent equal to $1/2$. Suppose what is being mea-

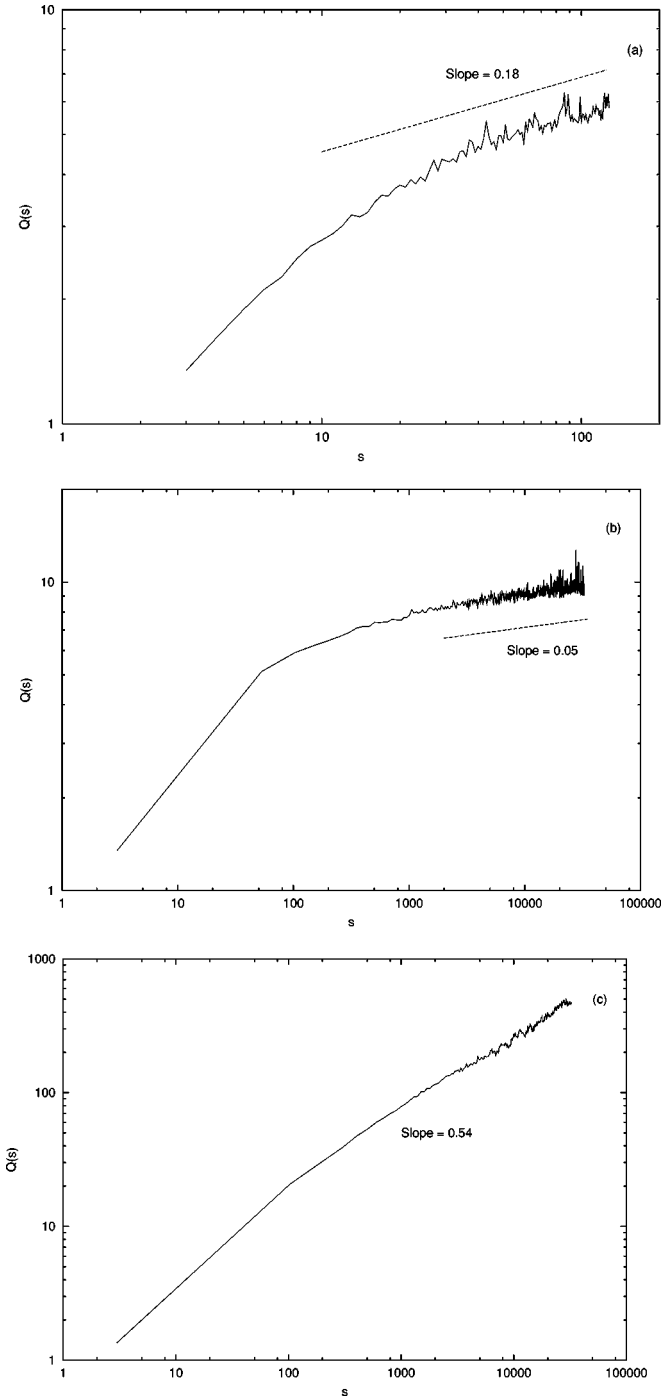


FIG. 14. (a) Log-log plot of the rescaled range statistic $Q(s)$ against the window size s for the velocity variable \dot{x} of a Langevin process with $\lambda = 5$ and 250 data points. (b) Same as above but with 60 000 data points. (c) Log-log plot of the rescaled range statistic $Q(s)$ against the window size s for the position variable x of a Langevin process with $\lambda = 5$ and 250 data points.

sured is not ξ_k but the differenced variable $\eta_k = \xi_{k+1} - \xi_k$. To see the effect of this, a Gaussian white noise process $\{\xi_k\}$ with zero mean and variance 0.25 was first generated. If the rescaled range analysis is performed on $\{\eta_k\}$, the result is shown in Fig. 13(a). The data length is 1024 points. If we force a linear fit to the end part of the log-log plot, we observe a Hurst exponent equal to about 0.12. However, this exponent is not a reflection of the process but is caused by the finite size of the data set. If we analyze a much longer

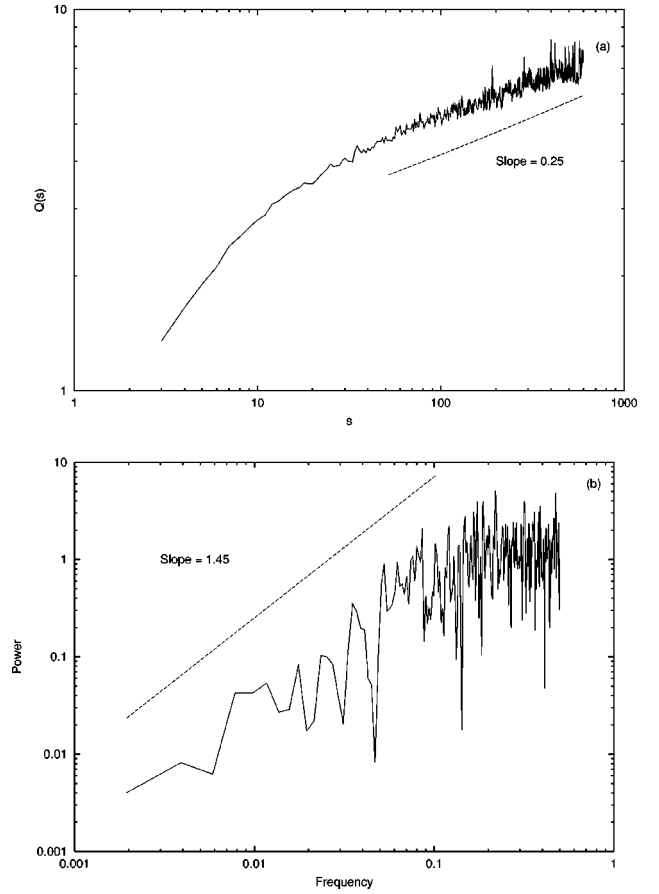


FIG. 15. (a) Log-log plot of the rescaled range statistic $Q(s)$ against the window size s for the interresponse interval time series data from the finger tapping experiment. (b) Spectral density of the same data.

data set (40 000 points), we observe that the slope of 0.12 that we had seen earlier is only a transient effect [see Fig. 13(b)]. It can be shown that the true slope goes to zero as the time lag s increases.

The H value of 0.12 obtained for the differenced data set of 1024 points can also be easily rejected by the integrated approach. Subjecting the same data set to the spectral analysis yields $\alpha = -1.95$ [Fig. 13(c)]. This value is totally inconsistent with the $\alpha = -0.76$ predicted by Eq. (14) based on $H = 0.12$. This inconsistency should be used as a clue to further examine the nature of the data set.

3. Langevin equation

In this section, we consider a more physical example—the Langevin equation. The Langevin process that we studied is

$$\dot{x} = -\lambda x + \xi(t), \quad (24)$$

where $\xi(t)$ is a white noise process with zero mean and variance 0.25 and $\lambda = 5$. The above stochastic differential equation was integrated using an efficient algorithm [19].

Suppose that the variable being measured is the velocity \dot{x} , and successive values of \dot{x} by the numerical integration scheme constitute our data set. The rescaled range analysis applied to a short data set of 250 points yields a Hurst exponent equal to 0.18 [see Fig. 14(a)]. On the other hand, if the

size of the data set is increased to 60 000 points, the value of H becomes nearly zero for large s values [Fig. 14(b)].

Theoretically, it can be shown that x , after an initial transient, is a stationary fundamental process. To demonstrate this we apply rescaled range analysis to the values of x . In this case, even for short data sets, we obtain a value of H close to 0.5 [see Fig. 14(c)], as predicted by theory. The result seen in Fig. 14(a) is therefore a consequence of \dot{x} being an overdifferenced variable.

4. Finger tapping data

Generally, we suggest that when a $H < 1/2$ is obtained from a random walk type of analysis, one should also perform a spectral analysis on the same data set. If the result is inconsistent with Eq. (14), then one should conclude that this data set is not from a fundamental process and partial sums of this data set should instead be considered for an analysis of the correlation properties.

As an example, we again consider the finger tapping experiment [7] described in Sec. II B. But now we analyze the interresponse intervals (IRI's) instead of the synchronization errors. The IRI's can be obtained from the synchronization error data by differencing it [7] and is itself an important physiological variable. Rescaled range analysis of this IRI time series data appears to give a value of $H = 0.25$ [see Fig. 15(a)]. But this is an artifact of the finite data size. This can be seen by performing a spectral analysis on the same IRI data [see Fig. 15(b)]. We see that this gives results inconsistent with Eq. (14). Thus the H value obtained in Fig. 15(a) is a consequence of the IRI being an overdifferenced variable, combined with finite data size and only one type of method.

IV. SUMMARY

Suppose that the autocorrelation function $C(s)$ for a stationary process scales with s as $C(s) \sim s^{-\beta}$. Depending on the values of β and the behavior of $\sum_{s=-\infty}^{\infty} C(s)$ we have the following classification for the process: (1) if $0 < \beta < 1$, we have $1/2 < H < 1$, and the process is said to have long range persistent correlation or long memory [9]. (2) If $1 < \beta < 2$ and $\sum_{s=-\infty}^{\infty} C(s) = 0$, we have $0 < H < 1/2$ and the process is said to have long range antipersistent correlation or anticorrelation. (3) If $\beta > 1$ and $\sum_{s=-\infty}^{\infty} C(s) \neq 0$ we have $H = 1/2$, and the process is said to have short range correlation. It is worth noting in this classification processes with $1 < \beta < 2$ can be classified as either having long range anticorrelation or short range correlation depending whether $\sum_{s=-\infty}^{\infty} C(s)$ is zero. We preserve the long range anticorrelation terminology, in keeping with the traditional naming of such processes. The main goal of this work has been to demonstrate the importance of the integrated approach, combining both spectral and random walk analyses, to the assessment of correlation behavior in time series data. We showed that the consistent use of both spectral and random walk analyses is not only essential in revealing the true nature of a given process, it can also prevent the false conclusion of long range correlation resulting from artifacts or wrong measurement variables combined with just one type of analysis method.

ACKNOWLEDGMENTS

This work was supported by US ONR Grant No. N00014-99-1-0062. G.R. thanks the Center for Complex Systems and Brain Sciences, Florida Atlantic University, where this work was performed, for hospitality.

-
- [1] B.B. Mandelbrot and J.R. Wallis, *Water Resour. Res.* **4**, 909 (1968); B.B. Mandelbrot and J.W. Van Ness, *SIAM Rev.* **10**, 422 (1968).
- [2] C.W.J. Granger, *Econometrica* **34**, 150 (1966).
- [3] M. Cassandro and G. Jona-Lasino, *Adv. Phys.* **27**, 913 (1978).
- [4] P.M. Richards, *Phys. Rev. B* **16**, 1393 (1977).
- [5] H.E. Hurst, *Trans. Am. Soc. Civ. Eng.* **116**, 770 (1951); H.E. Hurst, R.P. Black, and Y.M. Simaiki, *Long-term Storage: An Experimental Study* (Constable, London, 1965).
- [6] G. Matheron and G. De Marsily, *Water Resour. Res.* **16**, 901 (1980).
- [7] Y. Chen, M. Ding, and J.A. Scott Kelso, *Phys. Rev. Lett.* **79**, 4501 (1997). See the references cited in this paper for many other examples of long range correlated processes.
- [8] G. Rangarajan and D.A. Sant, *Geophys. Res. Lett.* **24**, 1239 (1997).
- [9] J. Beran, *Statistics for Long-memory Processes* (Chapman & Hall, New York, 1994).
- [10] For a random walk type of analysis other than the rescaled range method, see C.K. Peng, S.V. Buldyrev, M. Simons, H.E. Stanley, and A.L. Goldberger, *Phys. Rev. E* **49**, 1685 (1994); J.J. Collins and C.J. De Luca, *Exp. Brain Res.* **103**, 151 (1995); M.S. Taqqu, V. Teverovsky, and W. Willinger, *Fractals* **3**, 785 (1995).
- [11] C. Chatfield, *The Analysis of Time Series: An Introduction*, 4th ed. (Chapman & Hall, London, 1989).
- [12] A. Zygmund, *Trigonometric Series* (Cambridge University Press, New York, 1979).
- [13] W.H. Press, S.A. Teukolsky, W.T. Vetterling, and B.P. Flannery, *Numerical Recipes in Fortran*, 2nd ed. (Cambridge University Press, New York, 1992).
- [14] We comment that consistency here is defined in a rather loose fashion. In the future we will use more rigorous statistical criteria to provide the basis for evaluating whether the estimates from the two methods are consistent with Eq. (14).
- [15] R.B. Davies and D.S. Harte, *Biometrika* **66**, 153 (1987).
- [16] D.C. Boses and J.D. Salas, *Water Resour. Res.* **14**, 135 (1978); R.N. Bhattacharya, V.K. Gupta, and E. Waymire, *J. Appl. Probab.* **20**, 649 (1983).
- [17] J. Theiler, S. Eubank, A. Longtin, B. Galdrikian, and J.D. Farmer, *Physica D* **58**, 77 (1992).
- [18] C.W.J. Granger, *J. Econometrics* **14**, 150 (1980).
- [19] N.J. Rao, J.D. Borwankar, and D. Ramkrishna, *SIAM J. Control* **12**, 124 (1974); R. Mannella and V. Paleschi, *Phys. Rev. A* **40**, 3381 (1989).